Simulating beam-shape effects in non-collinear second harmonic generation

Simulación de efectos de perfil de haz en generación de segundo armónico no colineal

Benjamín Alonso[(1,*)], Javier R. Vázquez de Aldana[(1)], Luis Roso[(1,2)]

1. Departamento de Física Aplicada, Universidad de Salamanca, P. de la Merced s/n, 37008 Salamanca (Spain).

2. Centro de Láseres Pulsados Ultracortos Ultraintensos, CLPU, 37008 Salamanca, (Spain).

[(*)] Email: b.alonso@usal.es

Recibido / Received: 31/12/2008. Versión revisada / Revised version: 17/02/2009. Aceptado / Accepted: 25/02/2009

ABSTRACT:

We present a simplified model for the simulation of Second Harmonic Generation (SHG) with two fundamental beams that propagate in different directions: non-collinear SHG. In spite of its simplicity (diffraction is not included and the slowly varying envelope approximation in space is assumed) it can be used in many realistic situations. It has been implemented on Mathematica and is freely available to the reader. Beam-shape effects, conversion efficiencies, input intensity, phase-matching and other parameters can be studied with our code in a virtual experiment. We have applied the model to SHG of 1064 nm radiation in KDP crystal as an example.

Key words: Nonlinear Optics, Second Harmonic Generation, Non-Collinear, Simulation.

RESUMEN:

Se presenta un modelo sencillo para la simulación de la Generación de Segundo Armónico (SHG) en el caso en que los dos haces fundamentales se propagan en distinta dirección: SHG no colineal. A pesar de su simplicidad (no incluye difracción y se asume aproximación de envolvente lentamente variable en el espacio), se puede usar en muchas situaciones realistas. Se ha implementado en Mathematica y está disponible para el lector. En un experimento virtual, nuestro código permite estudiar efectos de perfil del haz, eficiencia de conversión, intensidad de entrada, ajuste de fases y otros parámetros. Como ejemplo, hemos aplicado el modelo a la SHG de radiación de 1064 nm en un cristal KDP.

Palabras clave: Óptica No Lineal, Generación de Segundo Armónico, No Colineal, Simulación.

REFERENCES AND LINKS

[1] P. Franken, A. Hill, C. D. Peters, G. Weinreich, "Generation of optical harmonics", *Phys. Rev. Lett.* **7**, 118-119 (1961).

[2] J. Giordmaine, "Mixing of light beams in crystals", *Phys. Rev. Lett.* **8**, 19-20 (1962).

[3] J. A. Armstrong, N. Bloembergen, J. Ducuing, P. S. Pershan, "Interactions between light waves in a nonlinear dielectric", *Phys. Rev.* **127**, 1918-1939 (1962).

[4] C. Méndez, J. R. Vázquez de Aldana, G. A. Torchia, L. Roso, "Integrated-grating-induced control of second-harmonic beams in frequency-doubling crystals", *Opt. Lett.* **30**, 2763-2765 (2005).

[5] F. Zernike, J. E. Midwinter, *Applied Nonlinear Optics*, John Wiley & Sons, New York (1973).

[6] J. M. Cabrera, F. Agulló, F. J. López, *Óptica Electromagnética*, Vol. II, Addison Wesley, Madrid (2000).

[7] R. W. Boyd, *Nonlinear Optics*, Academic Press, Boston (1992).

[8] Y. Shen, *The Principles of Nonlinear Optics*, Wiley, New York (1984).

[9] B. E. A. Saleh, M. C. Teich, *Fundamentals of Photonics*, pp. 100-107, John Wiley & Sons, New York (1991).

[10] G. Indebetouw, T. Zukowski, "Nonlinear optical effects in absorbing fluids: some undergraduate experiments", *Eur. J. Phys.* **5**, 129-134 (1984).

[11] I. Ruddock, "Nonlinear optical second harmonic generation", *Eur. J. Phys.* **15**, 53-58 (1994).

[12] V. G. Dmitriev, G. G. Gurzadyan, N. D. Nikogosyan, *Handbook of Nonlinear Optical Crystals*, Springer, Heidelberg (1991).

[13] K. Yang, S. Tripathy, J. Kumar, "Generalized expressions of effective nonlinear optical coefficient for non-collinear phase matching in uniaxial and cubic media", *Mol. Cryst. Liq. Crys. B: Nonlinear Opt.* **19**, 31-49 (1998).

[14] R. Bronson, E. J. Bredensteiner, *Schaum's Outline of Differential Equations*, pp. 104-111, McGraw-Hill, USA (2003).

[15] M. Abramowitz, I. A. Stegun, *Handbook of Mathematical Functions with Formulas, Graphs, and Mathematical Tables*, p. 896, Dover, New York (1974).

[16] P. Pliszka, P. P. Banerjee, "Nonlinear transverse effects in second-harmonic generation," *J. Opt. Soc. Am. B* **10**, 1810-1819 (1993).

1. Introduction

Nonlinear processes have been broadly studied in different areas of physics. In particular, Second Harmonic Generation (SHG) is one of the most basic processes in nonlinear optics, arising when a laser beam intense enough propagates through certain optical materials. Since the first studies [1-2], SHG has attracted a lot of interest due to the possibility to generate laser beams oscillating at new frequencies otherwise unavailable. Frequency doubling of laser beams is nowadays a very well established technique that is used for many practical applications. The simplest experimental setup involves only one incident fundamental beam that converts its frequency to the second harmonic (collinear SHG). In practice, only a few materials are convenient for SHG because of the propagation effects: the incident laser (at the fundamental frequency) and the second harmonic beam (with frequency two times that of the fundamental) will propagate, in general, with different phase velocities due to the dispersive properties of the nonlinear medium. This mismatch of the phase velocities is responsible for the destructive interference of the second harmonic waves generated at different points of the propagation direction that finally kills the generated second harmonic at a given propagation length. As it has been widely studied, the condition on the same phase acquired during the propagation (known as phase matching) is necessary to have efficient frequency conversion. Nowadays the concept of phase matching is experimentally settled by using different polarizations in anisotropic materials (the ordinary and the extraordinary, playing with the crystal axes orientation respect to the propagation to match their indexes), quasi-phase-matching [3] or the geometries where several (non-collinear) fundamental beams are involved [4].

In the non-collinear SHG the angle between beams can be used to achieve the phase matching, as will be seen below, which opens an alternative to the use of anisotropic crystals. The use of non-collinear geometries is thus necessary in many practical situations. For instance, it allows the intrinsic spatial separation of the fundamental and the second harmonic because they propagate in different directions (the SHG can be easily selected with a diaphragm). In more complex experiments, it can play the role of a spectrometer since it select a wavelength for each length when working with thick crystals. Moreover, if studying other second order nonlinear processes (such as sum or difference frequency generation), it is common having mandatory non-collinear configurations.

In many situations of interest, the theoretical study of the process requires numerical simulation. Many sophisticated models of SHG from continuous beams to ultra-short pulses have been developed in this context leading to successful results when comparing to experiments. Both collinear and non-collinear cases have been solved including all kind of corrections, for instance diffraction, dispersion of the refractive index or group-velocity dispersion. The concept of phase matching has been deeply studied and understood. Most of these sophisticated models are very computationally demanding and hardly accessible because of its complexity. On the other side, SHG with monochromatic and collinear plane waves can be described in a straightforward way under certain approximations, as it is done in most reference books [5-7]. More advanced books describe more complex processes and situations [8]. In this sense,

analytical expressions can be obtained assuming perfect phase matching or in the low conversion limit (undepleted pump). However, to our knowledge, there is a wide gap between SHG with plane monochromatic waves and more realistic cases.

The aim of this paper is to present an easy way to analyze SHG for monochromatic waves considering transverse effects and non-collinear geometries (the spatial profile of the two fundamental input beams is arbitrary). As in most of the numerical models, the slowly varying envelope approximation (SVEA) in space is assumed. Although it is fundamental, the effect of diffraction is not included in the propagation because of the characteristics of the model. However, it can be thought to be realistic in many practical situations where large unfocused (or loosely focused) beams are involved, beams that are nowadays available with intensity large enough to produce frequency conversion. Thus, we will assume that the beam propagates without divergence along the crystal length (typically with thicknesses of about a few millimeters). The model is freely available (attached to the publication) and can be easily modified by introducing different transverse modes (Laguerre-Gaussian and Hermite-Gaussian beams [9]), peak intensities, length and nonlinear susceptibility of the crystal and other parameters. The algorithms could be also extended to pulsed beams, but taking into account the time dependence is far from the scope of this work. This method is much simpler than other models used in investigation including all relevant effects both in time and in space, but on the contrary, it is simple, transparent, it can be fast understood and used in many situations, yielding meaningful results. Moreover, it gives us the chance of checking different inputs when trying to get a certain output. The problem equations are proposed including the first nonlinear term of the polarization (quadratic effects). After manipulations we found three coupled equations in first order partial derivatives. Therefore, we adapted standard numerical algorithms to integrate such equations where the field is propagated in subsequent planes.

Due to the relevance of nonlinear optics in many applications, the inclusion of simple experiments in undergraduate laboratories is becoming more and more important [10,11]. The model and the software presented in our work are proposed to be a virtual experiment on nonlinear optics very suitable for undergraduate level. The students are expected to learn the mentioned fundamental concepts of nonlinear optics and to familiarize with simulation and numerical algorithms. An undergraduate level of optics is required in the students before using this material.

2. Phase matching in uniaxial crystals

The most common procedure for achieving phase matching in SHG is to make use of the birefringence (dependence of the refractive index on the direction of polarization) of anisotropic crystals. In particular, uniaxial crystals like KDP (KH_2PO_4), are widely used in this context. In this section, we briefly discuss the general physics of uniaxial crystals applied to achieving phase matching for SHG. The particular case of a KDP crystal used to generate the second harmonic of a λ_ω=1.064 μm laser beam ($\lambda_{2\omega}$=0.532 μm) will be given as example.

In non-collinear geometries, the two fundamental waves will be assumed to propagate inside the crystal with angles ±α respect to the *z*-axis (without loss of generality), in the plane *x*-*z*, thus resulting in second harmonic beam propagating along the *z*-axis as it can be seen in Fig. 1 (note that outside the crystal both fundamental beams will propagate with a larger angle respect to the z-axis in agreement with Snell's law).

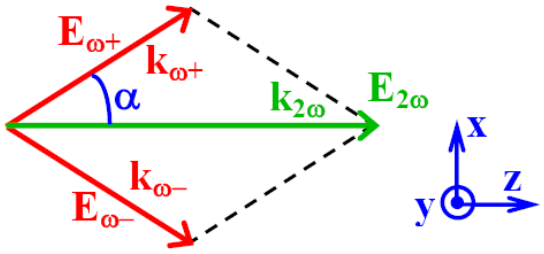

Fig. 1. Geometry involved in the non-collinear SHG.

The diagram of Fig. 1 shows, in fact, the phase matching condition for any parametric process like SHG: the sum of the wave vectors of the incoming (fundamental) waves must be equal to the wave vector of the generated wave (second harmonic), that is $\mathbf{k}_{2\omega}=\mathbf{k}_{\omega+}+\mathbf{k}_{\omega-}$. From this vectorial condition we get $k_{2\omega}=\cos\alpha\,(k_{\omega+}+k_{\omega-})$ and finally the following condition for the refractive indices: $2n_{2\omega}=(k_{\omega+}+k_{\omega-})\cos\alpha$. It can be experimentally achieved by choosing a suitable angle α in non-

collinear SHG or by matching the fundamental and second harmonic indexes in collinear SHG thanks to the material birefringence. Both cases will be discussed below.

Uniaxial crystals are characterized by having a particular axis with different refractive index, known as the optic axis of the crystal. This causes that a plane wave will propagate with different refractive index depending on the direction of propagation of the phase (given by its wave vector $\vec{k}$). In these crystals, light can propagate with two different behaviours: ordinary and extraordinary. The ordinary wave, polarized in the plane orthogonal to the optic axis (isotropy plane), travels with a refractive index n_o, whereas the effective refractive index for the extraordinary wave (with polarization perpendicular to the ordinary wave) depends on the propagation direction (see, for instance, [6,7])

$$n_e^2(\theta) = \frac{n_e^2 n_z^2}{n_e^2 \sin^2(\theta) + n_z^2 \cos^2(\theta)}. \qquad (1)$$

where θ is the angle between the wave vector and the optic axis, and the indexes n_z and n_o are the principal values of the refractive indexes of the crystal. Notice that we have called n_z=n_e(θ=90º), the refractive index for the extraordinary wave when its phase propagates perpendicular to the optic axis of the crystal. On the other hand, when the angle is θ=0º (parallel to the optic axis), the extraordinary index is n_o and the wave propagates like the ordinary one. As a result, the ordinary and the extraordinary waves have different polarization.

In the particular case of KDP, the principal values of the refractive indices for λ_ω=1.064 μm and $\lambda_{2\omega}$=0.532 μm can be calculated from the Sellmeier equations [12]:

$$\begin{aligned} n_{o,\omega} &= 1.4942, \quad n_{z,\omega} = 1.4603, \\ n_{o,2\omega} &= 1.5129, \quad n_{z,2\omega} = 1.4709. \end{aligned} \qquad (2)$$

Depending on the role played by the fundamental or the second harmonic, two types of phase matching are defined. When both fundamental waves are ordinary or extraordinary, the phase matching process is named type-I. When the fundamental waves have the opposite polarization (one is ordinary and the other extraordinary), the phase matching process is named type-II.

We will focus our work on type-I phase matching with both fundamental waves having ordinary polarization (thus, the generated second harmonic will be extraordinary). The optic axis of the crystal will be contained in the plane defined by the direction of propagations of the waves. Due to birefringence, the wave vector and the energy (Poynting vector) of the extraordinary wave (the second harmonic) will propagate inside the crystal along slightly different directions [6,7,12]. The angle between phase and energy propagation is named walk-off angle and can be calculated from

$$\theta_{walk-off} = \theta_{2\omega} - \theta, \qquad (3)$$

with $\theta_{2\omega}$ defined as $\tan\theta_{2\omega} = n_{o,2\omega}^2 n_{z,2\omega}^{-2} \tan\theta$.

The nonlinear effect is produced by a non-zero second order susceptibility $\chi^{(2)}$ in the material giving induced nonlinear polarization. The nonlinear propagation increases with this susceptibility, which is responsible for the SHG. Typically, the effective nonlinear coefficient d_{eff} defined as $2d_{eff}=\chi^{(2)}$ is used instead.

The effective nonlinear coefficient d_{eff} of the frequency conversion depends on the experiment geometry and it is related to the known parameters of the crystal. The expression in a crystal class $\bar{4}$2m (point group) is the following [13]

$$d_{eff} = -d_{36} \sin(\theta_{2\omega}) \sin(\phi_{\omega+} + \phi_{\omega-}). \qquad (4)$$

where $\theta_{2\omega}$ is the angle between the optic axis of the crystal and Poynting vector of the second harmonic wave, and $\phi_{\omega+}$ is the azimuthal angle of the wave $E_{\omega+}$ respect to the crystal axes starting at positive x-axis. We assume that the crystal has been cut in the best situation to produce nonlinear second order effects, that is, when the azimuthal angles with the crystal axes are $\phi_{\omega+}=\phi_{\omega-}=\pi/4$.

The nonlinear coefficient is taken from the literature [12] and is d_{36}(1.064 μm)=0.39 pm/V. Since we are working in the CGS system of units, we have to convert it to the appropriate units using the ratio 1 statVolt=299.8 V, thus the coefficient used is $d_{36}=1.17\times10^{-8}$ cm/statVolt.

First of all, in the non-collinear SHG, we use the angle between incident beams directions to achieve the phase matching condition (or at least small phase mismatch experimentally) so we can obtain the phase matching angle α_{PM} given by $\cos\alpha_{PM}=n_{e,2\omega}(\theta)/n_{o,\omega}$. Moreover, we consider that the optic axis angle of the crystal is θ=90º because the effective nonlinear coefficient will be the maximum and the second harmonic (extraordinary

wave) will not have walk-off (see Fig. 2(a)). Then, the desired parameters are:

$$n_{e,2\omega}(\theta) = n_{z,2\omega} = 1.4709; \quad \theta_{2\omega} = 90^{o};$$
$$d_{eff} = -1.17\times10^{-8} \text{ cm/statVolt}; \qquad (5)$$
$$\alpha_{PM} = 10.132^{o}.$$

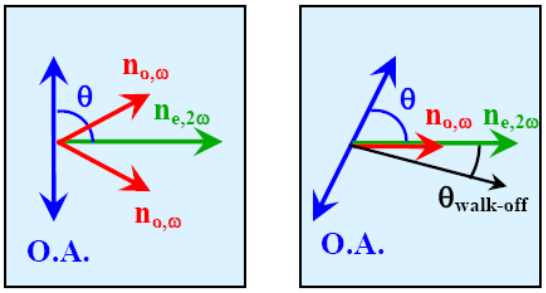

a) Non-collinear b) Collinear

Fig. 2. Optic axis (O.A.) orientation and beam propagation direction in non-collinear (a) and collinear (b) geometry. The walk-off angle gives the direction of Poynting vector for collinear second harmonic (due to the particular choice of the O.A. orientation in the non-collinear setup the walk-off is zero in this case.) The indices shown in the scheme represent the refraction indices experienced by each wave.

Concerning the collinear situation, the variable used to reach collinear phase matching is the angle of the optic axis respect to the propagation (see Fig. 2(b)). Since we are solving type I generation where the extraordinary wave is second harmonic, the angle can be calculated from the phase matching condition $n_e^2\left(\theta_{coll}^{PM}\right) = n_{o,\omega}^2$, and is given by [7]

$$\sin^2\left(\theta_{coll}^{PM}\right) = \frac{n_{o,\omega}^{-2} - n_{o,2\omega}^{-2}}{n_{z,\omega}^{-2} - n_{z,2\omega}^{-2}} \Rightarrow$$
$$\Rightarrow \theta_{coll}^{PM} = 41.255^{o}. \qquad (6)$$

Assuming again that the crystal has been designed in the most favourable situation, we have $\phi_{\omega+}=\phi_{\omega-}=\phi_{\omega}=\pi/4$ and the angle of the optic axis is θ_{coll}^{PM}, so the parameters take the values

$$n_{e,2\omega}(\theta) = n_{o,2\omega} = 1.4942;$$
$$\theta_{2\omega} = 42.860^{o}; \qquad (7)$$
$$d_{eff} = -7.95\times10^{-9} \text{ cm/statVolt}.$$

In this case, the second harmonic has an angular walk-off $\theta_{walk\text{-}off}$=1.604º, calculated from Eq. (3). We have kept a precision of 0.001º for the angles in these calculations just for convenience. The precision required in lab experiments for the angles is difficult to assess provided that it is strongly dependent on several parameters as the monochromaticity of the fundamental wave, the divergence of the beam or the crystal length (in standard goniometers the precision is usually much smaller, typically $0^{o}10' = 0.17^{o}$).

If the phase matching condition is not exactly satisfied, the power of the generated second harmonic signal will dramatically decrease. This effect is accounted for through the phase mismatch, defined as $\Delta\vec{k} = \vec{k}_{\omega+} + \vec{k}_{\omega-} - \vec{k}_{2\omega}$, that projected along the propagation direction of the second harmonic gives $\Delta k = k_{\omega+}\cos\alpha + k_{\omega-}\cos\alpha - k_{2\omega}$. It can be shown [6,7] that, in the low conversion limit (undepleted pump) in collinear geometry and considering plane monochromatic waves, the SHG intensity depends with the phase mismatch as

$$I_{2\omega} \propto I_{\omega}^2(0)\cdot L^2 \cdot \text{sinc}^2\left(\frac{\Delta k \cdot L}{2\pi}\right), \qquad (8)$$

where L is the crystal length (fixed), $I_{\omega}(0)$ is the fundamental intensity input and the sinc-function is defined as $\text{sinc}(x)=\sin(\pi x)/(\pi x)$. This function has a maximum when $\Delta k=0$ and oscillates between zero and secondary maxima (see Fig. 3). The first zero around the main maximum appears at $\Delta k=\pm 2\pi/L$. For a given SHG geometry with perfect phase matching, if the wavelength of the fundamental beam or the phase matching angle slightly changes, then Δk changes accordingly and the conversion efficiency decreases. Since the first zero position is proportional to L^{-1}, the spectral and angular admittances (range of wavelengths and phase matching angles for which the SHG efficiency drops to 0.5 of the maximum value) are larger for shorter crystal lengths. On the other hand, the efficiency is also proportional to L^2, so the optimum crystal length for a given experiment must be found as a commitment between efficiency and admittances. Finally, notice that the SHG intensity depends on $I_{\omega}^2(0)$, so it increases nonlinearly (as expected) with the fundamental intensity. An analogous expression to Eq. (8) can be found for non-collinear SHG and, therefore, the above considerations can be extended to this case.

3. Model

3.a. Fields and set out

The proposed problem has been set out considering incident beams with arbitrary transverse modes and a defined propagation direction in the crystal, so we have to solve equations with the three spatial variables.

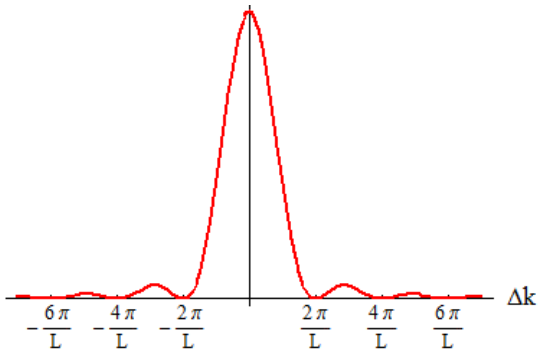

Fig. 3. Second harmonic intensity as a function of the phase mismatch: sinc-function.

In order to simplify the final expressions of the equations, we define $\boldsymbol{\varepsilon}_{\omega\pm}$ (fundamental beams corresponding to angles $\pm\alpha$, see Fig. 1) and $\boldsymbol{\varepsilon}_{2\omega}$ (the second harmonic) as the complex envelopes of the fields (that is, the electric fields except for the temporal and the rapidly oscillating spatio-temporal phase) that only depend on the position $\mathbf{r}=\{x,y,z\}$:

$$\begin{aligned} \mathrm{E}_{\omega\pm}(\mathrm{r},t) &= \varepsilon_{\omega\pm}(\mathrm{r})e^{i[k_\omega(\pm x\sin\alpha+z\cos\alpha)-\omega t]}; \\ \mathrm{E}_{2\omega}(\mathrm{r},t) &= \varepsilon_{2\omega}(\mathrm{r})e^{i[k_{2\omega}z-2\omega t]}. \end{aligned} \tag{9}$$

In the particular case of collinear SHG the angle is $\alpha=0$, condensing the definitions in

$$\begin{aligned} \mathrm{E}_{\omega}(\mathrm{r},t) &= \varepsilon_{\omega}(\mathrm{r})\exp\{i[k_\omega z-\omega t]\}; \\ \mathrm{E}_{2\omega}(\mathrm{r},t) &= \varepsilon_{2\omega}(\mathrm{r})\exp\{i[k_{2\omega}z-2\omega t]\}. \end{aligned} \tag{10}$$

3.b. Equations obtaining

In this study, we do not regard the vectorial character of the electric field, assuming that each field has the correct polarization according to the phase-matching conditions in the crystal (necessary in anisotropic materials). We will consider only type-I phase matching that means that the two fundamental beams have the same polarization, but can be directly extended to other cases. The system of units used is the CGS. We consider Maxwell's equations including the first nonlinear term associated to the second order susceptibility $\chi^{(2)}$, which is the responsible for the SHG. The resulting wave equation is

$$\nabla^2 E = \frac{\varepsilon}{c^2}\frac{\partial^2 E}{\partial t^2} - \frac{4\pi}{c^2}\frac{\partial^2 P_{NL}}{\partial t^2}, \tag{11}$$

where c is the speed of light. The dielectric permittivity $\varepsilon=1+\chi^{(1)}$ includes the first order susceptibility $\chi^{(1)}$ arising from the linear polarization term. In our scope, we have an equation for each wave with its corresponding nonlinear polarization term P_{NL}. In the non-collinear case, the nonlinear polarizations are given by [7]:

$$\begin{aligned} P_{\omega\pm} &= 2\chi^{(2)}E^*_{\omega\mp}E_{2\omega}e^{-i\omega t}, \\ P_{2\omega} &= 2\chi^{(2)}E_{\omega+}E_{\omega-}e^{-i2\omega t}. \end{aligned} \tag{12}$$

The second order susceptibility takes different values depending on the mix-frequency processes that it involves. From this moment, we define the second order susceptibility for the SHG process as $\chi^{(2)}\equiv\chi^{(2)}(\omega,\omega\rightarrow 2\omega)$. Obviously, it has been considered as a number not as a tensor (in anisotropic materials it is a tensor, but an effective scalar value is always used).

In the collinear interaction we consider that the fields $E_{\omega+}$ and $E_{\omega-}$ degenerate in only one called E_ω. Since it is physically necessary that the intensity of this wave is the sum of the fundamental non-collinear intensities when $\alpha=0$ (being each of that half the total intensity), the amplitude of the collinear fundamental wave will be the same except for a factor equal to the root square of two. This is the reason why the coefficient two disappears in the nonlinear polarization oscillating at double frequency (it is absorbed in the field amplitude):

$$\begin{aligned} P_{\omega} &= 2\chi^{(2)}E^*_{\omega}E_{2\omega}e^{-i\omega t}, \\ P_{2\omega} &= \chi^{(2)}(E_\omega)^2 e^{-i2\omega t}. \end{aligned} \tag{13}$$

Then, we introduce these considerations in the wave equations for the ω and 2ω fields, and we assume the following main approximations. The first assumption is the slowly varying envelope approximation (SVEA) in space. It consists of neglecting the second order spatial derivative of the envelopes along the propagation direction. It can be assumed in most of the situations in which homogeneous media are involved and no interface is present in the propagation. The second one supposes that the diffraction is negligible in the propagation length. It is reasonable for short propagation lengths and "soft" beam-shapes. This approach also implies that beams propagate without being strongly focused. The resulting equations that we have solved both in the non-collinear case and the collinear one are:

$$\begin{aligned} &\left(\pm\tan\alpha\frac{\partial}{\partial x}+\frac{\partial}{\partial z}\right)\varepsilon_{\omega\pm} = \\ &= -\frac{4i\chi^{(2)}\pi\omega^2}{c^2k_\omega\cos\alpha}\exp\{-iz\Delta k\}\varepsilon^*_{\omega\mp}\varepsilon_{2\omega}. \end{aligned} \tag{14a}$$

$$\frac{\partial \varepsilon_{2\omega}}{\partial z} = -\frac{16 i \chi^{(2)} \pi \omega^2}{c^2 k_{2\omega}} e^{+iz\Delta k} \varepsilon_{\omega+} \varepsilon_{\omega-}. \quad (14b)$$

where we have defined the phase mismatch $\Delta k = 2k_\omega \cos(\alpha) - k_{2\omega}$. The full derivation of the propagation equations can be found at the header of the Mathematica script. Notice the high symmetry of the equations involving the envelopes. The three coupled equations can be particularized to the collinear generation:

$$\begin{aligned} \frac{\partial \varepsilon_\omega}{\partial z} &= -\frac{4 i \chi^{(2)} \pi \omega^2}{c^2 k_\omega} e^{-iz\Delta k} \varepsilon_\omega^* \varepsilon_{2\omega}, \\ \frac{\partial \varepsilon_{2\omega}}{\partial z} &= -\frac{8 i \chi^{(2)} \pi \omega^2}{c^2 k_{2\omega}} e^{+iz\Delta k} (\varepsilon_\omega)^2. \end{aligned} \quad (15)$$

It is fundamental to realize that the sources of the nonlinear processes (the right-hand side of the equations) are modulated by a phase including the phase mismatch Δk. When this quantity is zero, both fundamental and generated waves propagate with the same phase velocity projection along the z-axis giving constructive interference. This is exactly the mentioned condition on the propagation velocity of the waves (phase matching condition), which implies the relation $n(\omega)\cos(\alpha)=n(2\omega)$. The nonlinear polarization terms are the source of the fields and become from the three essential processes that can produce the waves mixing in all possible directions, because the nonlinear process is reversible and depending on the phase matching conditions it can be energy returning to the fundamental waves from that converted to second harmonic (down-conversion).

We have dependence on the three spatial variables in the envelopes, but it is possible to recover the plane wave case assuming that the envelopes only depend on the z-coordinate. This problem has been solved in classical textbooks as Zernike *et al* [5] and many more since then. As it has been said in that simplified situation, analytical expressions can be found under certain conditions.

4. Solving method

4.a. Basic considerations

The final equations form a system of coupled equations in partial derivatives of first order. The philosophy of the algorithm is always to calculate the field distribution in a complete plane $z=z_0+\Delta z$ using the values of the electric-fields in the previous plane $z=z_0$. The crystal is sampled in a three-dimensional Cartesian grid. At the beginning, we used the Euler's method [14] of first order $f(x_0+\Delta x) \approx f(x_0)+\Delta x[\partial f(x_0)/\partial x]$, which can be easily applied to the field propagating along the z-axis. However, the derivatives of the incident beams (the fundamental beams) are with respect to a combination of the variables x and z. The way to propagate these fields is by means of the integration of the z-derivative (in the z-direction) and numerical approximation of the x-derivative as $\partial f(x_0)/\partial x \approx [f(x_0+\Delta x)-f(x_0)]/\Delta x$. The numerical integration of the equations is given by:

$$\varepsilon_{\omega\pm}(x_0, y_0, z_0 + \Delta z) \cong \left[\varepsilon_{\omega\pm}\right]_{(r_0)} \mp \Delta z \tan\alpha \left[\frac{\partial \varepsilon_{\omega\pm}}{\partial x}\right]_{(r_0)} - \Delta z \frac{4 i \chi^{(2)} \pi \omega^2}{c^2 k_\omega \cos\alpha} \exp\{-i\Delta k \cdot z_0\} \left[\varepsilon_{\omega\mp}^* \varepsilon_{2\omega}\right]_{(r_0)}. \quad (16a)$$

$$\varepsilon_{2\omega}(x_0, y_0, z_0 + \Delta z) \cong \left[\varepsilon_{2\omega}\right]_{(r_0)} - \Delta z \frac{16 i \chi^{(2)} \pi \omega^2}{c^2 k_{2\omega}} \exp\{+i\Delta k \cdot z_0\} \left[\varepsilon_{\omega+} \varepsilon_{\omega-}\right]_{(r_0)}. \quad (16b)$$

The effective nonlinear coefficient d_{eff} is commonly used instead of the second order nonlinear susceptibility $2d_{eff} \equiv \chi^{(2)}$. The fields have been made adimensional dividing by the envelope peak of one incident beam. Moreover, the procedure was improved in the non-collinear case by substituting the first order method for the second order Modified Euler's Method [14] (also known as trapezoidal formula [15]). To even more increase the accuracy without needing denser sampling (and longer calculation times), we use the 4th order Runge-Kutta method in the collinear case [14].

The beam width parameter (in the calculation) is taken to be high enough to completely include the transverse distribution of energy for both fundamental beams.

4.b. Initial conditions

We choose z as the direction in which the second harmonic beam propagates, being x the direction

containing the other component of the non-collinear beams and y the transverse direction. Before solving the differential equations that govern the process, we have to define the initial conditions, that is, the values of the electric fields at the beginning of the crystal ($z=z_{\min}$) for the whole transverse plane (initialize the fields). We consider that in the plane $z=z_{\min}$ only exits fundamental field. Although this is not a necessary condition that can be changed by the user, not having second harmonic input is the most common situation. Furthermore, in non-collinear SHG we need to change the coordinates from the incident beams intrinsic system to the coordinates described above and then impose the initial conditions at $z=z_{\min}$. We use Laguerre-Gaussian or Hermite-Gaussian beams [9] as input.

4.c. Control of the accuracy

In spite of implementing second and fourth order numerical methods, we must be very careful with the choice of the sampling in order to ensure the accuracy of the solution. The step size in z-direction must be small enough to avoid divergence in the Euler's method. This is roughly given by the condition:

$$\Delta z << \frac{l}{\chi^{(2)}\varepsilon_{\max}}, \qquad (17)$$

where we have used the definition $l=c^2k_\omega\cos\alpha/4\pi\omega^2$ and $\varepsilon_{\max}$ is the maximum value of the electric field reached at a certain point of the spatial sampling. Therefore, we know that the product between the adimensional magnitude $\chi^{(2)}\varepsilon_{\max}$ and the step $\Delta z/l$ will play the role of the necessary condition for the integration.

Additionally, the accuracy achieved by the calculation can be checked by testing the electric energy of the interacting waves. The total energy is proportional to

$$\left\langle \left| E_{\omega+} + E_{\omega-} + E_{2\omega} \right|^2 \right\rangle = \left| E_{2\omega} \right|^2 + \left| E_{\omega+} \right|^2 + \left| E_{\omega-} \right|^2 + 2\,\mathrm{Re}\left\{ \varepsilon_{\omega+}\varepsilon_{\omega-}^{*} e^{i2k_\omega \sin\alpha \cdot x} \right\}, \qquad (18)$$

and must remain constant from a z-plane to the following one. Due to the interference term between the two fundamental beams (note that they have the same polarization because type-I phase matching is considered) the total energy oscillates in the x-direction but its integral gives an average that is a constant. The period of such oscillations is $\pi/(k_\omega\sin\alpha)$, so we can check if the resolution of the sampling is high enough to describe it.

The total energy conservation is verified during the calculation and, if the step is not small enough, the program sends us a warning message to abort evaluation because calculations will be wrong. The conservation error limit is set by default to 1% from initial energy, but it can be manually changed.

5. Application to Second Harmonic Generation in KDP

5.a. KDP crystal and beam parameters

In order to show an application of the model, we use as incident beams the output of the Nd:YAG laser, with a fundamental wavelength λ_ω=1064 nm in the infrared and the green second harmonic $\lambda_{2\omega}$=532 nm. This conversion is very often used. Nd:YAG lasers produce pulses of typically few nanoseconds. The study of SHG with monochromatic waves is thus justified due the very long pulse duration.

The calculation of the optimum parameters of the non-collinear and collinear SHG is explained in detail in Section 2. The simulation considers type I generation. In non-collinear conversion, we assume that the angle of the optic axis respect to the second harmonic propagation is θ=90º. Such an angle means that the optic axis is perpendicular to the plane containing the three interacting beams (plane x-z). The refractive indexes are $n_{o,\omega}$=1.4942 and $n_{e,2\omega}(\theta)=n_{z,2\omega}$=1.4709, and the non-collinear angle for phase matching is α_{PM}=10.132º. The effective nonlinear coefficient results $d_{eff}=-1.17\times10^{-8}$ cm/statVolt.

On the other hand, in collinear generation the phase matching condition imposes θ=41.3º and $n_{e,2\omega}(\theta)=n_{o,\omega}$=1.4942. The effective nonlinear coefficient is $d_{eff}=-7.95\times10^{-9}$ cm/statVolt.

We obtain the maximum value of the complex envelope module for the incident beams from the peak intensity of the beams in the air. Then, we must convert it to CGS units

$$\left|\varepsilon_{\omega\pm}\right|_{\max}\left(\frac{\mathrm{statVolt}}{\mathrm{cm}^2}\right) = \frac{1}{299.8}\left(\frac{\mu_0}{\varepsilon_0}\right)^{1/4}\sqrt{2I_{\max}\left(\frac{\mathrm{W}}{\mathrm{cm}^2}\right)}, \qquad (19)$$

where we have considered the difference between the complex amplitude (that we use in the model) and the real field.

5.b. Non-collinear SHG with Gaussian beams

The fundamental waves are the Gaussian beams (mode 00 of the Laguerre-Gaussian beam [9]). In the non-collinear interaction, the point where fundamental beams crosses is taken as the origin of coordinates, and the problem is solved in a symmetric region containing the superposition zone where the nonlinear process takes place. Thus, the computation volume is determined from the incident beams width and the non-collinear angle α. The crystal dimensions in centimeters are $(0.28, 0.14, 0.8)$, respectively to (x,y,z)-directions, corresponding to a beam width 0.141 cm, and the integration step used is Δz=0.01 cm (ensuring the accuracy). The centers are separated a distance 0.143 cm (the product of the crystal length by $\tan\alpha$) at the entrance of the crystal. The peak intensity value is $I_{max}=6\times10^7$ W/cm^2, which implies $|\varepsilon_{\omega\pm}|_{max}$=709.2 statVolt/cm^2 according to Eq. (19). We intentionally use a non-collinear angle slightly different from α_{PM}, so there is a small phase mismatch $\Delta k=5.5\times10^{-6}$ cm^{-1}. The program implemented on Mathematica is attached to the online publication as Media 1.

In Fig. 4 the total energy of the three interacting waves is shown along the crystal (it is integrated in the y-direction). The centre of the two fundamental beams (propagating with angles $\pm\alpha$) crosses at z=0 and interference fringes can be seen where fundamental beams overlap, as predicted in Eq. (18). The interaction between both beams generates a second harmonic beam that propagates along the z-axis. As the two fundamental beams separate they carry much less energy due to the conversion to SHG.

The outputs of the program are the electric-field distributions over the whole sampling. Intensities, energies and phase-maps are calculated from these fields. We show as example the transverse intensity and phase distribution of the second harmonic for the parameters given above beam at different sections of the crystal in Fig. 5 (the entire video is available online as supplementary material: Media 2). The second harmonic intensity is wider in the y-direction. This asymmetric shape reflects the importance of the superposition zone: since the incident beams propagate with opposite x-components the main spatial superposition between both beams is achieved around x=0. Moreover, we can learn that the spatial phase varies faster in the y-direction than the x-direction, and its difference increases as the beam propagates.

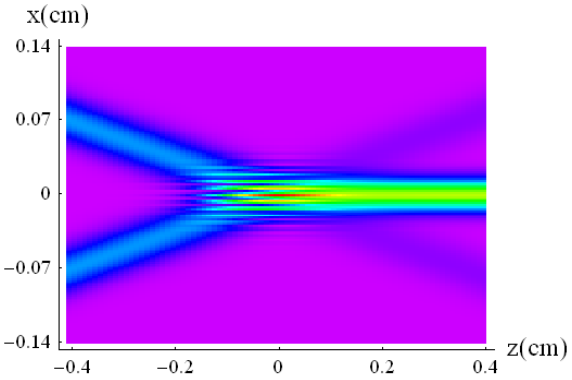

Fig. 4. Density of total electromagnetic energy integrated in y-direction.

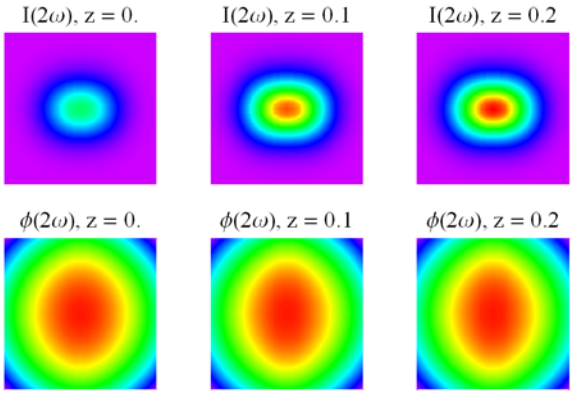

Fig. 5. Intensity (up) and phase (down) of the second harmonic at different sections of the crystal. The x-direction is the vertical axis and the y-direction is the horizontal axis.

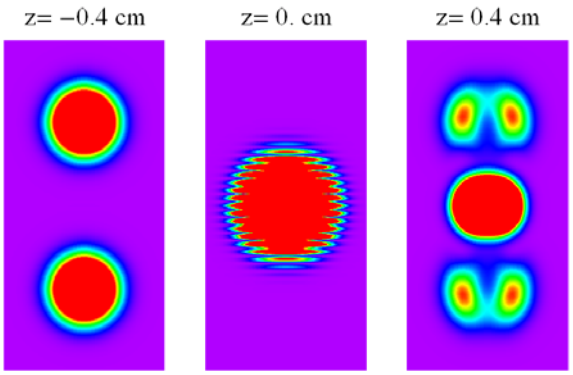

Fig. 6. Transverse distribution of the normalized total energy at the beginning of the crystal (left), at the centre (middle) and at the end (right). The maximum at the centers of the fundamental beams is caused by down-conversion (due to phase mismatch). The x-direction is the vertical axis and the y-direction is the horizontal axis.

This is more clearly represented in Fig. 6, where transverse distributions (sections at different z=constant planes) of the density of total electromagnetic energy are plotted (whole video attached online: Media 3). The section at the beginning of the crystal (left) shows the gaussian incident beams because initially there is not second harmonic wave. Then, both fundamental waves propagate and cross at the centre of the crystal (z=0), giving interference fringes near this point. In z=0 there is also the generated second harmonic (no oscillating contribution). The energy output is the remainder of the fundamental beams at the top and at the bottom, and the second harmonic leaving the crystal at the centre (see also Fig. 4).

5.c. Collinear SHG for Hermite-Gaussian mode 01

The incident wave is the mode 01 of the Hermite-Gaussian beams [9], which has a null minimum in the line y=0. In this case, the computation region is again symmetric respect to the origin of coordinates. The crystal length is 0.8 cm, and we have chosen a beam width 0.8 cm, and the integration step used is Δz=0.02 cm, which ensures the accuracy. The envelopes are normalized respect to the value $|\varepsilon_\omega|_{max}$=2895 statVolt/cm^2 that would give peak intensity I_{max}=10^9 W/cm^2 if it were the Hermite-Gaussian mode 00 (gaussian beam). We induce a considerable phase mismatch Δk=0.176 cm^{-1} arising from an angle of the optic axis of the crystal different from θ_{PM}. The Mathematica program corresponds to Media 4.

Transverse sections of second harmonic intensity at different positions of the crystal are represented in Fig. 7 (video available online: Media 5). The phase mismatch causes the change in the direction of the energy conversion, alternating from fundamental to second harmonic and vice versa. Since second harmonic generation is a nonlinear process, it occurs faster where the initial electric field is higher, leading to an earlier change from up-conversion to down-conversion at the two maxima of the incident beam, which produces the ring structure at each lobe of the beam. These phenomena have already been simulated with more complicated models [16] including diffraction and obtaining similar results.

The effect of the beam shape on phase mismatch is clearly shown if we represent the propagation along the nonlinear material (section x=0) as seen in Fig. 8. The maxima and minima reflect the different rates of the conversion (referred to the propagation direction z) caused by the initial transverse distribution of energy.

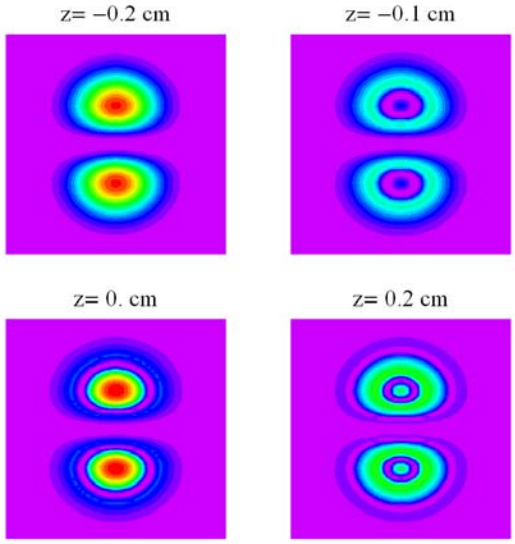

Fig. 7. Transverse sections of second harmonic intensity. The phase mismatch causes the change in the direction of the energy conversion alternating from fundamental to second harmonic waves. The x-direction is the vertical axis and the y-direction is the horizontal axis.

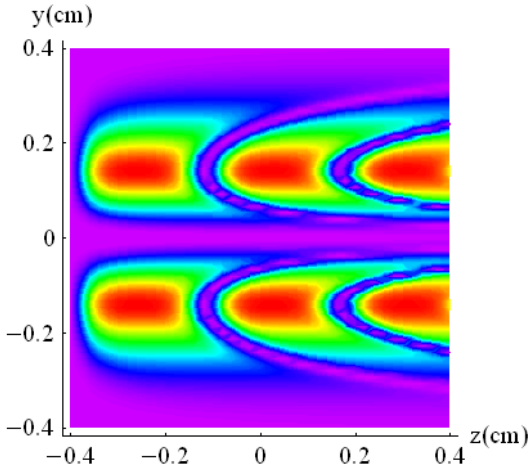

Fig. 8. Second harmonic intensity at a section x=0.

6. Conclusions

We have presented an algorithm for non-collinear second harmonic generation with monochromatic waves. The main assumptions of the model (slowly varying envelope approximation in space and diffraction negligible) allow a reasonably simple treatment of the problem but it remains useful in many practical applications. Effects of the transverse beam shape, intensity, phase matching,

crystal length and nonlinear properties, can be easily understood with the code. We propose the use of such code as virtual experiment on nonlinear optics that could be very suitable for undergraduate level. The students are expected to learn fundamental concepts of nonlinear optics and to familiarize with simulation and numerical algorithms.

The program is not very computationally demanding and can be run on typical desktop computers without specific hardware requirements. This is one of the goals of our simplified model. Fast calculations can be done with durations in the order of a couple of minutes.

Acknowledgements

This work was funded by the Spanish Ministry of Science and Education (Projects No. FIS2006-04151 and No. CSD00C-07-24113). Benjamín Alonso is grateful to the Spanish Ministry of Science MICINN for the financial support.

